AN1471

Efficiency Analysis of a Synchronous Buck Converter using Microsoft® Office® Excel®-Based Loss Calculator

Author: *Joseph Depew*
Microchip Technology Inc.

INTRODUCTION

Efficiency versus cost is always a trade-off when designing a switch mode power supply, with synchronous buck converters being no exception.

The large variety of discrete components that are on the market today offer the designer a nearly infinite number of solutions. This, combined with tight schedules and budgets, increases the need for a fast and accurate way to predict the performance of a system. Ideally, these predictions begin before a circuit is built, to reduce the number of design iterations that are needed to provide an optimized solution. As part of an optimized solution, the designer must verify that the design meets efficiency and cost requirements, without exceeding temperature constraints of lossy components.

The goal of this application note is to provide designers of synchronous buck converters with a fast and accurate way to calculate system power losses, as well as overall system efficiency. The majority of power losses in a typical synchronous buck converter (Figure 1) occur in the following components:

- High-Side MOSFET
- Low-Side MOSFET
- Inductor
- MOSFET driver

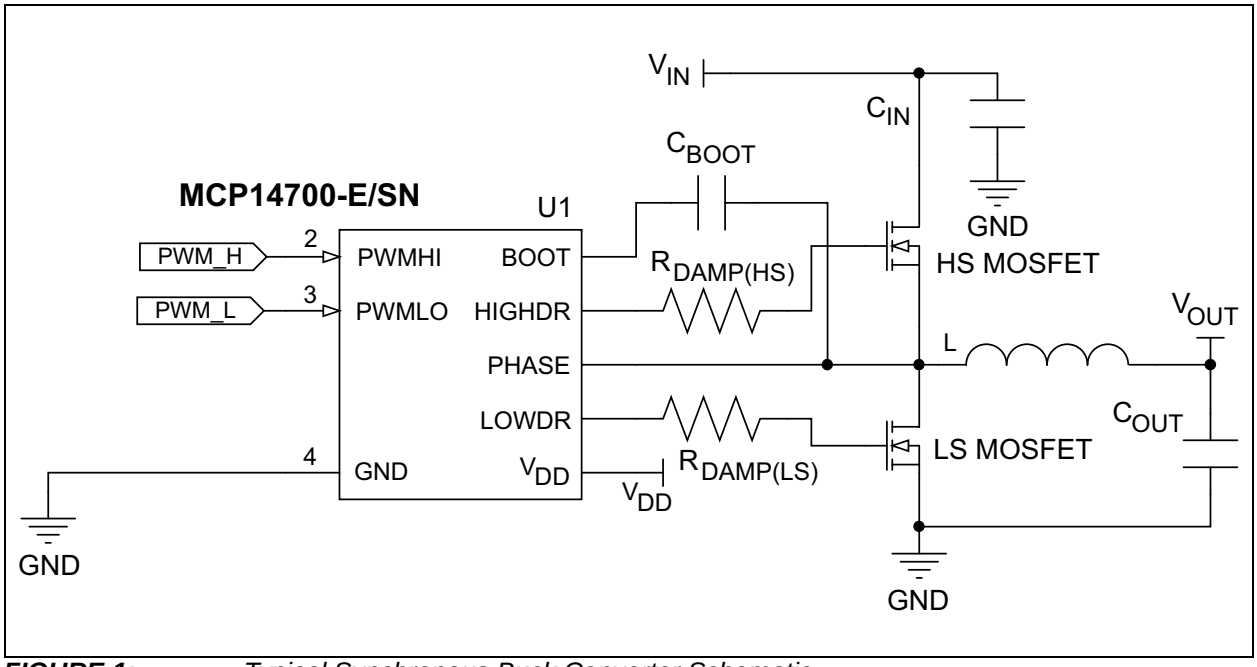

FIGURE 1: *Typical Synchronous Buck Converter Schematic.*

HIGH-SIDE MOSFET LOSSES

The total power loss in any MOSFET can be summed up as the losses due to conduction, and the losses due to switching. In a low-duty cycle, converter switching losses will tend to dominate for a MOSFET in the high-side position. The duty cycle for a buck converter is described as:

$$DC = \frac{V_{OUT}}{V_{IN}}$$

Where:

V_{OUT} = System Output Voltage
V_{IN} = System Input Voltage

When the duty cycle is low, the high-side switch will be on for a small percentage of the period. The drain of the high-side MOSFET is tied to V_{IN}, while the source is tied to the phase node, as shown in Figure 1. When the high-side turn on begins, the phase node is clamped below ground by the body diode of the low-side MOSFET. This large voltage differential from drain-to-source, in addition to the fact that the high-side MOSFET is also switching the full load current of the converter, leads to a lossy switching event.

High-Side Conduction Losses

Conduction losses in a high-side MOSFET are described as:

EQUATION 1:

$$P_{HS(COND)} = R_{DS(ON)} \times I_{DS(RMS)}^2$$

Where:

$R_{DS(ON)}$ = Drain-to-Source On Resistance
$I_{DS(RMS)}$ = RMS Drain-to-Source Current

Note that the $I_{DS(RMS)}$ term is squared in this calculation. Therefore, as load current increases and as the duty cycle gets higher, the conduction losses may exceed the switching losses.

The calculation for RMS drain-to-source current, as well as inductor ripple current, can be found in **Appendix C: "Additional Equations"**. Since $R_{DS(ON)}$ is dependant on the junction temperature of the device, and losses will increase the junction temperature, an iterative calculation is necessary. These iterations must be performed until the junction temperature of the device stabilizes (generally to <1%).

High-Side Switching Losses

Figure 2 is a graphical representation of the switching losses in the high-side MOSFET. Note that these are ideal waveforms, and assume a constant gate current.

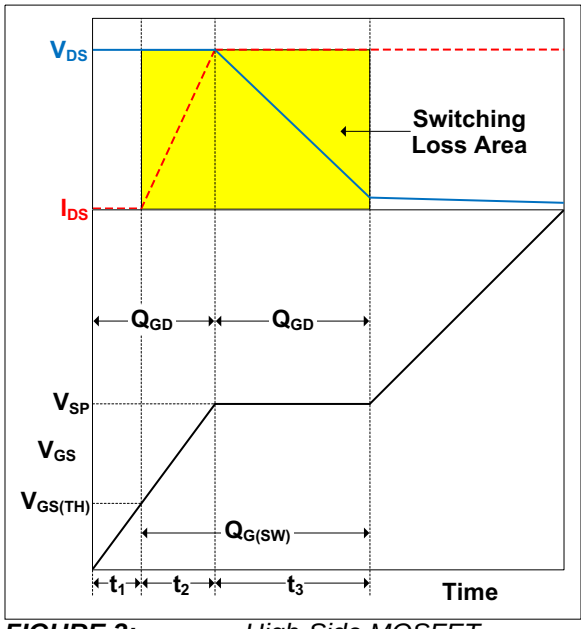

FIGURE 2: *High-Side MOSFET Switching Waveforms.*

The initial rise period t_1 of V_{GS} (the MOSFET's gate-to-source voltage) occurs when the MOSFET driver begins to supply current to the MOSFET's gate. During this time, the input capacitance C_{ISS} (C_{GS} + C_{GD}) is being charged, while V_{DS}, the MOSFET's drain-to-source voltage, remains constant. A diagram of a MOSFET's parasitic capacitances is shown in Figure 3. There is no drain-to-source current flow at this time. Therefore, there are no switching losses during this period.

At the beginning of period t_2, the V_{GS} voltage exceeds the gate-to-source threshold voltage ($V_{GS(TH)}$). Current will begin to flow from drain-to-source, while C_{ISS} continues to charge. This current will rise linearly until I_{DS} equals the inductor current I_L. Since there is a voltage drop across the MOSFET equal to V_{IN}, and current I_{DS} is flowing through the device, there are significant switching losses during this period.

During period t_3, the I_{DS} current remains constant, while the V_{DS} voltage begins to drop. While the drain-to-source voltage is dropping, nearly all of the gate current is delivered to charge C_{GD}. Since almost no gate current is used to charge C_{GS}, the gate-to-source voltage remains relatively flat at a voltage called the "switch-point" voltage (V_{SP}). This region is commonly known as the Miller Plateau. During this period, similar to t_2, there is a voltage drop from drain-to-source, as well as significant current flowing through the device. Therefore, t_3 is a lossy period of the switching cycle.

Upon exiting period t_3, the MOSFET channel is enhancing, up to the point where V_{GS} reaches its maximum value. Switching losses have ceased, and conduction losses occur until the high-side MOSFET is turned off. The turn-off event is very similar, happening in reverse of the turn-on event.

The power loss during the switching cycles of the high-side MOSFET can be described as:

EQUATION 2:

$$P_{HS(SWITCH)} = \frac{V_{IN} \times I_{OUT}}{2} \times F_{SW} \times (t_{S(LH)} + t_{S(HL)})$$

Where:

V_{IN} = Input Voltage
F_{SW} = Switching Frequency
$t_{S(LH)}$ = Switching Time, Low-to-High
$t_{S(HL)}$ = Switching Time, High-to-Low

The switching times from low-to-high and high-to-low can be calculated using Equations 3 and 4:

EQUATION 3:

$$t_{S(LH)} = \frac{Q_{G(SW)}}{I_{DRVR(LH)}}$$

Where:

$Q_{G(SW)}$ = Gate Charge, Switching
$I_{DRVR(LH)}$ = Driver Current, Low-to-High

EQUATION 4:

$$t_{S(HL)} = \frac{Q_{G(SW)}}{I_{DRVR(HL)}}$$

Where:

$I_{DRVR(HL)}$ = Driver Current, High-to-Low

The $Q_{G(SW)}$ parameter can be found using the V_{GS} versus Q_G characterization graph that can be found in the MOSFET's data sheet (see Figure 2). It is the charge required to bring the V_{GS} from $V_{GS(TH)}$ to the end of the Miller Plateau. $Q_{G(SW)}$ can also be found if $Q_{G(TH)}$ is listed as a data sheet parameter, using Equation 5:

EQUATION 5:

$$Q_{G(SW)} = (Q_{GS} + Q_{GD}) - Q_{G(TH)}$$

Driver currents for each transition are described in Equations 6 and 7:

EQUATION 6:

$$I_{DRVR(LH)} = \frac{V_{DD} - V_{SP}}{R_{DR(PU)} + R_G + R_{DAMP}}$$

Where:

V_{DD} = Driver Voltage
V_{SP} = Switch Point Voltage
$R_{DR(PU)}$ = Driver Pull-Up Resistance
R_G = MOSFET Gate Resistance
R_{DAMP} = External Damping Resistance

EQUATION 7:

$$I_{DRVR(HL)} = \frac{V_{SP}}{R_{DR(PD)} + R_G + R_{DAMP}}$$

Where:

$R_{DR(PD)}$ = Driver Pull-Down Resistance

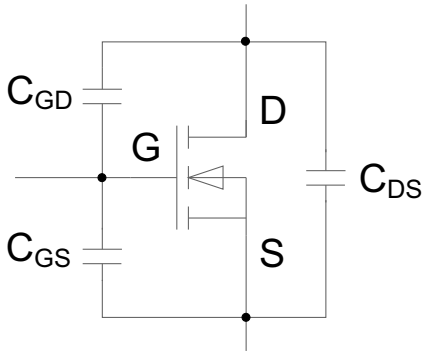

$C_{ISS} = C_{GD} + C_{GS}$
$C_{OSS} = C_{GD} + C_{DS}$
$C_{RSS} = C_{GD}$

FIGURE 3: *MOSFET Parasitic Capacitances.*

Other High-Side MOSFET Switching Losses

Although conduction and switching loss account for a majority of power losses in the high-side MOSFET, there are other minor lossy areas in the switching cycles. One of these areas of loss is the power lost due to charging the gate of the MOSFET, expressed as:

EQUATION 8:

$$P_{GATE} = Q_{G(TOTAL)} \times V_{DD} \times F_{SW}$$

Where:

$Q_{G(TOTAL)}$ = Total Gate Charge

Note that $Q_{G(TOTAL)}$ will change with respect to V_{GS}, so be sure to pick the value from the data sheet that corresponds with the MOSFET driver's gate drive voltage (V_{DD}). These losses will be distributed among all resistances in the gate drive path, including the MOSFET driver pull-up or pull-down resistance (depending on which edge is being evaluated), the series damping resistor (R_{DAMP}) and the gate resistance of the MOSFET (R_G).

Another area of loss in a synchronous buck converter is the reverse recovery loss of the low-side MOSFET's body diode. Note that this power loss will occur in the high-side MOSFET, as it is the turn on of this device that has to recover the low-side's body diode. The charge required to recover the body diode can be found in the MOSFET's data sheet, under diode characteristics, labeled Q_{RR}. These losses can be described as:

EQUATION 9:

$$P_{DIODE(RR)} = Q_{RR} \times V_{IN} \times F_{SW}$$

Where:

Q_{RR} = Body Diode Reverse Recovery

Finally, during each switching cycle, the output capacitance C_{OSS} ($C_{GD} + C_{DS}$) of both the low-side and high-side MOSFET must be charged. These losses can be approximated by the following equation:

EQUATION 10:

$$P_{COSS} = \frac{(COSS_{LS} + COSS_{HS}) \times (V_{IN})^2 \times F_{SW}}{2}$$

Where:

$COSS_{LS}$ = LS MOSFET Output Capacitance

$COSS_{HS}$ = HS MOSFET Output Capacitance

LOW-SIDE MOSFET LOSSES

Looking back at Figure 1, it can be seen that the low-side MOSFET's drain is tied to the phase node, while the source is connected to ground. When the high-side device turns off, and before the low-side MOSFET is turned on, the body diode in the low-side MOSFET will begin to conduct, as current through the inductor must continue to flow. Since the source of the low-side device is tied to ground, the phase node must go below ground by a voltage equal to the forward drop of the body diode, in order to conduct. Therefore, when the low-side switch is turned on, there is only a voltage equal to the forward drop of the body diode across it. This leads to a "soft" switching event, with losses that are considered negligible in this application note.

As with the high-side MOSFET, the losses in the low-side MOSFET are largely dependant on duty cycle and RMS current. Conduction losses, both from drain-to-source while the device is on, and from source-to-drain through the body diode when both MOSFETs are off, completely dominate in a low-side application.

Low-Side Conduction Losses

Similar to conduction losses in the high-side device, the conduction losses in the low-side MOSFET can be calculated with the following equation:

EQUATION 11:

$$P_{LS(COND)} = R_{DS(ON)} \times I_{DS(RMS)}^2$$

Since the duty cycle in synchronous buck converters tends to be low, the drain-to-source RMS current in the low-side MOSFET can become quite high. At high-load currents, the conduction losses in the low-side device can become the largest area of loss in a buck converter. As with the high-side MOSFET calculations, the conduction losses in the low-side device require an iterative calculation, in order to provide accurate results.

As explained earlier, the body diode of the low-side MOSFET will turn on when both switches are off in a synchronous buck converter. During this time, known as Dead Time (DT), conduction losses will occur in the body diode. These losses can be described as:

EQUATION 12:

$$P_{DIODE} = DT \times F_{SW} \times V_{SD} \times I_{OUT}$$

Where:

DT = Dead Time, Rising and Falling

V_{SD} = Diode Forward Voltage

Note that the DT in this equation accounts for both the rising and falling edges combined. At low-load currents, it is common to see the diode conduction losses equal to, or greater than, on-time conduction losses in the low-side MOSFET.

Low-Side MOSFET Gate Charge Losses

Another component of power loss in the low-side MOSFET, although small, is the power lost charging the gate. This loss is calculated using the same formula used for the high-side device (see Equation 8).

INDUCTOR LOSSES

In a synchronous buck converter operating at high-load currents, the equivalent series resistance of the winding of an inductor will have a significant impact on system efficiency. This impact can be described as:

EQUATION 13:

$$P_{INDUCTOR} = ESR_L \times I_{OUT}^2$$

Where:

ESR_L = Inductor Equivalent Series Resistance

Note that this power loss is not dependant on the duty cycle, since the inductor is always conducting. Inductor selection is critical when optimizing a synchronous buck converter, as power loss in the inductor can rival losses in the MOSFETs, when the load current is high.

Core losses will not be discussed in this application note, as the calculations can become complex. These losses can usually be considered negligible, when compared to the inductor's conduction loss.

MICROSOFT OFFICE EXCEL-BASED LOSS CALCULATOR FOR SYNCHRONOUS BUCK CONVERTERS

Although the equations for losses in a buck converter are well documented and straightforward, going through each of the calculations by hand can be extremely time consuming. This is especially true if calculations for multiple load ranges, voltages and devices are performed. In order to aid system designers of synchronous buck converters, a Microsoft Office Excel-based loss calculator is now available for download from Microchip's web site. This calculator allows designers to store large numbers of MOSFETs, inductors and MOSFET drivers for evaluation. It also calculates power losses and efficiencies from 0A up to the designer's maximum load current, in a user-defined step size. The output of this calculator provides a table of values for each of the losses in the system, along with system efficiency and die temperature for the two MOSFETs. Finally, an efficiency graph is generated, in order to give the user an idea of the system's performance over a range of load currents. The layout and operation of this calculator is described in detail in **Appendix B: "Microsoft Office Excel-based Loss Calculator Layout and Operation"**.

In order to show the validity of the calculator, the losses and overall efficiency of a synchronous buck converter, with the parameters from Table 1, will be calculated using the loss calculator. The results of these equations are shown in Table 2.

TABLE 1: EXAMPLE OF SYSTEM PARAMETERS

Parameter	Symbol	Value	Units
Input Voltage	V_{IN}	12	V
Output Voltage	V_{OUT}	1.2	V
Load Current	I_{OUT}	20	A
Switching Frequency	F_{SW}	300000	Hz
Driver V_{DD}	V_{DD}	5	V
Ambient Temperature	T_A	25	°C
High-Side MOSFET		**MCP87050**	
Low-Side MOSFET		**MCP87022**	
MOSFET Driver		**MCP14700**	
Inductor		XAL1010-102MEB	
High-Side Damping Resistance	$R_{DAMP(HS)}$	2	Ω
Low-Side Damping Resistance	$R_{DAMP(LS)}$	2	Ω

TABLE 2: LOSS CALCULATOR RESULTS

Parameter	Value	Units
HS Conduction Loss	.2725	W
LS Conduction Loss	1.0047	W
HS Switching Loss	.9979	W
Diode Conduction Loss	.1536	W
Reverse Recovery Loss	.1260	W
Output Cap Loss	.0339	W
HS Gate Drive Loss	.0188	W
LS Gate Drive Loss	.0390	W
Inductor Winding Loss	.4400	W
Output Power	24.0000	W
Input Power	27.0864	W
Efficiency	88.61	%
HS Die Temperature	95.09	°C
LS Die Temperature	73.65	°C

Hand calculation using the formulas in this application note will result in the same values as shown in Table 2. Figure 4 is a pie chart, which shows the percentage of total system losses occurring in each area of loss explained in this application note. Notice how high-side MOSFET switching losses and low-side MOSFET conduction losses account for ~65% of the losses in the system. This chart shows that, for this system in particular, switching losses dominate in the high-side position, while conduction losses dominate in the low-side position. Also note that the high-side MOSFET is the lossiest component in this system, followed by the low-side MOSFET, then the inductor.

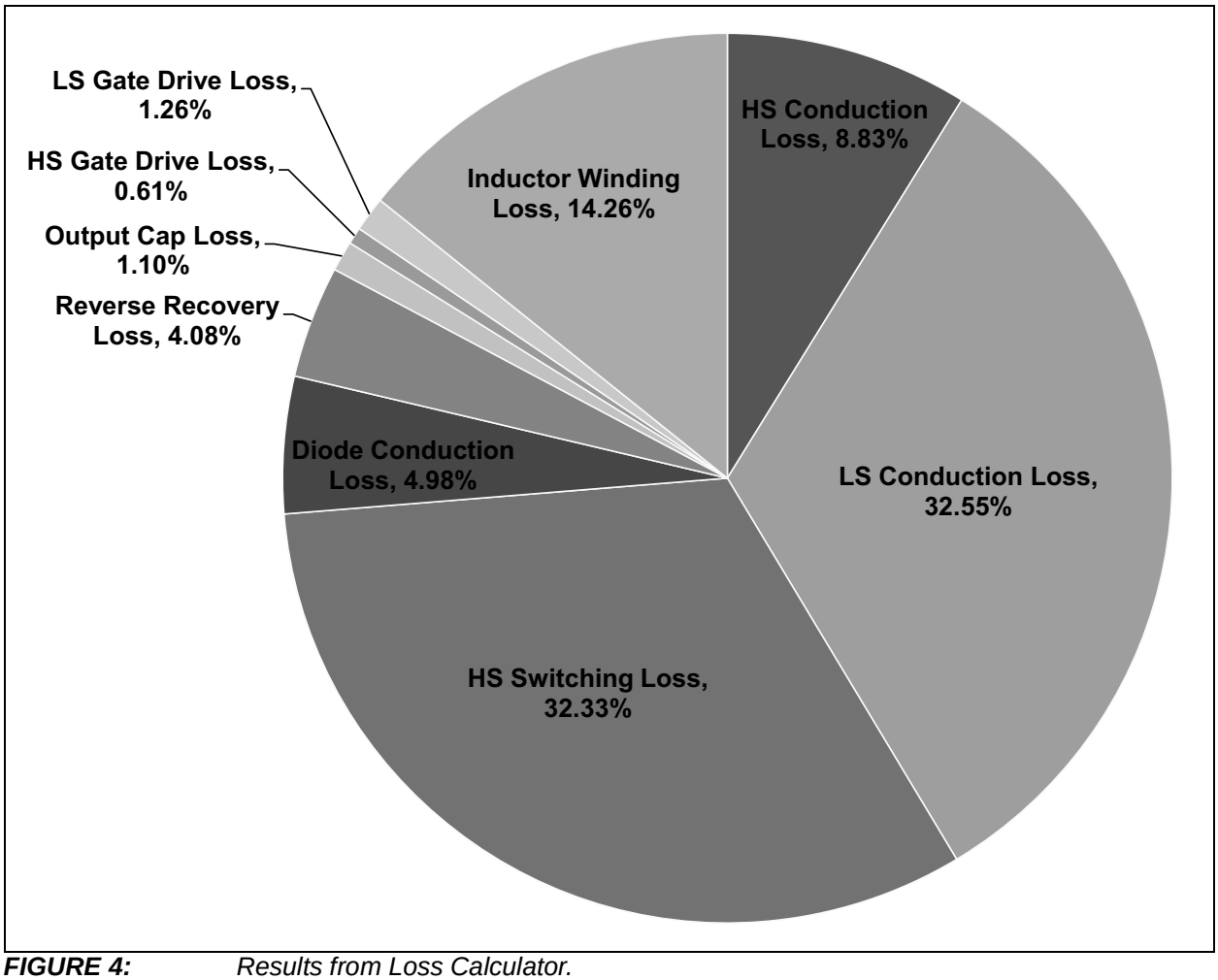

FIGURE 4: *Results from Loss Calculator.*

CONCLUSION

In order to show the accuracy of the loss calculator, a circuit was built with the parameters shown in Table 1. The system efficiency was measured using an automated test setup. The test setup takes input voltage and current measurements, along with output voltage and current measurements, in order to provide an efficiency curve from 1A - 20A, in 1A steps. Sufficient dwell time is allowed between measurements to allow the die temperatures of the MOSFETs to stabilize. The measured results are compared to calculated results in Figure 5. In this figure, the shape of the measured and calculated efficiency curves follow each other well, but there is a slight offset between them. This offset is generally caused by three things:

- board design
- various negligible losses
- measurement error

When a printed circuit board is designed, the placement of the components and the interconnects between them can have a significant impact on system operation and efficiency. This is especially true as switching frequency and load current increase. The copper traces on the circuit board add parasitic inductance and capacitance to a system, resulting in losses that are often challenging and time consuming to calculate. Component packaging is another area that can add parasitics to a system. Also, the close proximity of power components to one another can lead to a heating effect, increasing power losses. An example of this is that a pair of hot MOSFETs located close to an inductor can raise the temperature of the inductor, raising its ESR, creating more power loss. These additional losses are not accounted for in this application note, and are a large part of the difference between the calculated and measured efficiencies for this system.

As stated earlier, the switching losses in the low-side MOSFET, as well as the core losses in the inductor, are assumed to be negligible in this application note. Other areas of power loss, although very small relative to the losses discussed in this application note, include losses in the system's input and output capacitors and the additional power loss in the inductor as it heats up. It is important to note that an iterative calculation was not used when calculating inductor losses, so losses may increase as the temperature rises. When combined, all of these small areas of loss can lead to significant system-level power losses.

Measurement accuracy also has an effect on the calculated results. All power supplies, multimeters, electronic loads and shunt resistors used to operate and measure the system can have a small amount of error, especially when used in conjunction with the long leads necessary for hooking up the circuit board.

Although there are slight differences between the calculated and measured values, the efficiency curves are still very useful to a designer. Using these curves, changes can be made to a system in order to optimize the solution quickly and efficiently.

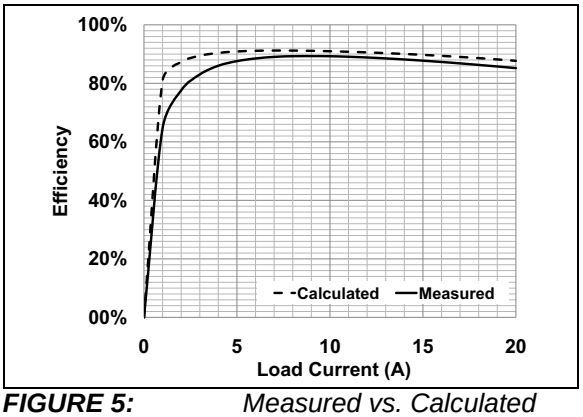

FIGURE 5: *Measured vs. Calculated Results.*

REFERENCES

- Anderson, L.B. and Anderson, R.L. - *"Fundamentals of Semiconductor Devices"*, McGraw-Hill, ©2005.
- Mohan, N., Undeland, T.M. and Robbins, W.P. - *"Power Electronics: Converters, Applications, and Design"*, John Wiley & Sons, ©2003
- Pressman, A.I., Billings, K. and Morey, T. - *"Switching Power Supply Design"*, McGraw-Hill, ©2009.

APPENDIX A: ENABLING MACROS IN MICROSOFT OFFICE EXCEL

The loss calculator discussed in this application note requires macros in order to perform many functions. Therefore, macros must be enabled in Microsoft Office Excel in order to allow the loss calculator to operate. Instructions on enabling macros for Excel 2003 and 2007 versions are included below.

A.1 Excel® 2003

In order to enable macros in Excel 2003, follow these steps:

1. Go to the Tools menu.
2. From the list, select “Macro”.
3. Select “Security”.
4. Select the “Medium” option.
5. Press **OK**.

A.2 Excel® 2007

In order to enable macros in Excel 2007, follow the steps:

1. Press the **Office** button located in the upper left corner.
2. Click on the **Excel Options** button at the bottom of the menu.
3. In the Excel Options dialog, select “Trust Center” from the left panel.
4. Press the **Trust Center Settings** button on the right panel.
5. From the Trust Center window, choose “Macro Settings” from the left panel.
6. Select “Enable all macros....”
7. Press **OK** to complete the settings.

APPENDIX B: MICROSOFT OFFICE EXCEL-BASED LOSS CALCULATOR LAYOUT AND OPERATION

B.1 Loss Calculator Layout

The Loss Calculator tool contains eight sheets:

- **Instructions** - shows steps to enable macros in Excel, describes in brief the sheets in the tool and defines the MOSFET parameters
- **Graph** - this sheet shows the efficiency curves that are generated during the calculations in the **Operating Conditions** sheet. Previous curves are left on the graph unless "Auto Clear Charts" is selected or the **Clear Charts** button is pressed.
- **GraphData** - this sheet displays all of the actual data that is graphically displayed on the **Graph** sheet. This allows the user to add in other efficiency curves with the same step size, as well as compare measured efficiency curves with calculated efficiency curves. All system parameters are listed on this sheet for each curve, making the comparison between curves easier.
- **Efficiency** - this sheet shows all of the system losses that are calculated when the **RUN** button is pressed, in addition to the overall system efficiency. The conduction losses are calculated using an iterative calculation involving RDS(on) and die temperature. This calculation assumes a linear relationship between RDS(on) and junction temperature.
- **Operating Conditions** - the main sheet of the tool, where the user inputs all the operating conditions and device parameters of the power supply. The MOSFETs, drivers and inductors can be selected from their respective sheets.
- **MOSFETs** - lists all of the MOSFETs that are currently available in the spreadsheet. The user can add any MOSFET to this sheet. To select a MOSFET for use on the **Operating Conditions** sheet, right-click the Part Number and choose "Select as HS MOSFET..." or "Select as LS MOSFET..."
- **Drivers** - This sheet lists all of the MOSFET drivers that are currently available in the spreadsheet. The user can add any MOSFET driver to the list. To select a MOSFET Driver for use on the **Operating Conditions** sheet, right-click the part number and choose "Select as Driver..."
- **Inductors** - This sheet lists all of the inductors that are currently available in the spreadsheet. The user can add any inductor to this sheet. To select an inductor for use on the **Operating Conditions** sheet, right-click the part number and choose "Select as Inductor..."

B.2 Operating the Tool

When opening the loss calculator, the **Operating Conditions** sheet of the workbook is displayed. This is essentially the control panel for the calculator (see Figure B-1). The user enters all of the operating conditions of the system here, including input voltage, output voltage, maximum load current, step size, switching frequency, driver V_{DD}, ambient temperature and damping resistances. The high and low-side MOSFETs, MOSFET driver and inductor can be selected from their respective sheets in the workbook. In order to select a component, go to that component's sheet, right-click anywhere on the row of the device you wish to select, and choose "Select as [*device type*]...". The device will automatically be added to the **Operating Conditions** sheet, as shown in Figure B-1.

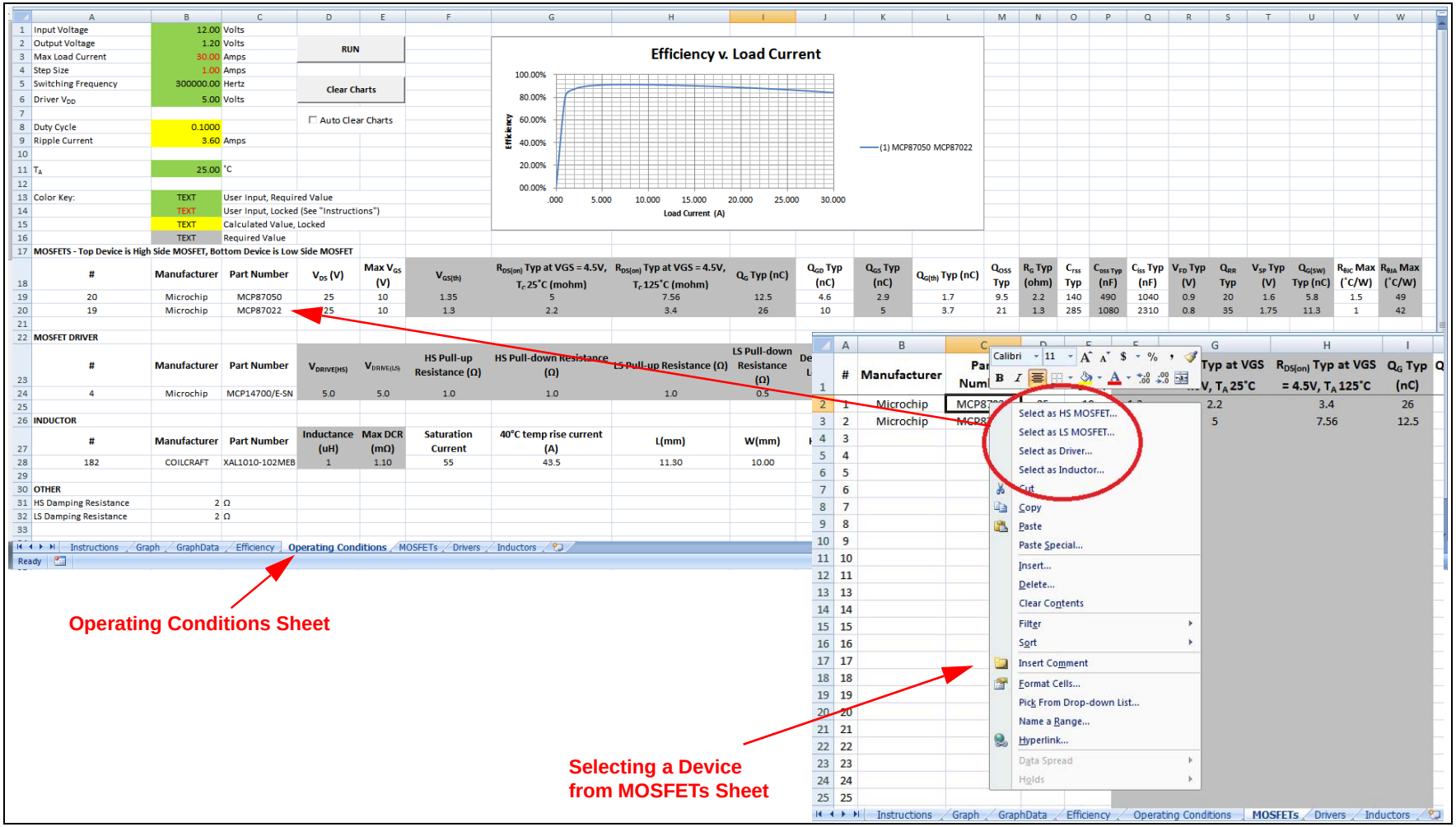

FIGURE B-1: OPERATING CONDITIONS WORKSHEET AND HOW TO SELECT A DEVICE OPERATION.

The **Operating Conditions** sheet contains the following buttons:

- **RUN**
- **Clear Charts**
- **Auto Clear Charts** checkbox.

The **RUN** button starts the main macro, which calculates all of the system losses and efficiency, based on the user's parameters. This macro also generates two efficiency graphs, one on the **Operating Conditions** sheet, and a full-size graph on the **Graph** sheet. The user can run as many combinations of parts as desired, and all of the efficiency data will stay on the graphs, stored on the **GraphData** sheet. Allowing the user to store multiple efficiency curves on the same graph makes evaluating the impact on the system from a component change quick and easy. The **GraphData** sheet also stores all of the vital system parameters in a group of cells for reference. This feature allows the user to review what components and parameters were entered to generate each efficiency curve. Figure B-2 shows a screenshot of the **GraphData** sheet with multiple efficiency curves. The difference between the two curves comes from using two different inductors in a system, with all other parameters being the same.

When the user wishes to clear the data, the **Clear Charts** button will clear all data from the two graphs, as well as the data from the **GraphData** sheet. Optionally, the user can leave the **Auto Clear Charts** box checked, which will clear the graph data upon every press of the **RUN** button.

Another item of note on the **Operating Conditions** sheet is that when there is data showing on the graphs, the "Maximum Load Current" and the "Step Size" cells are locked. This is to ensure that all successive curves placed on the graphs have the same resolution and number of steps. Clearing the charts via the **Clear Charts** button unlocks these cells.

The calculator will not run if all the necessary values are not filled in on the **Operating Conditions** sheet. For the system parameters, all of the cells must be populated. For the devices, all of the cells needed to run have a gray background. All other cells are optional, but provide important information about the devices.

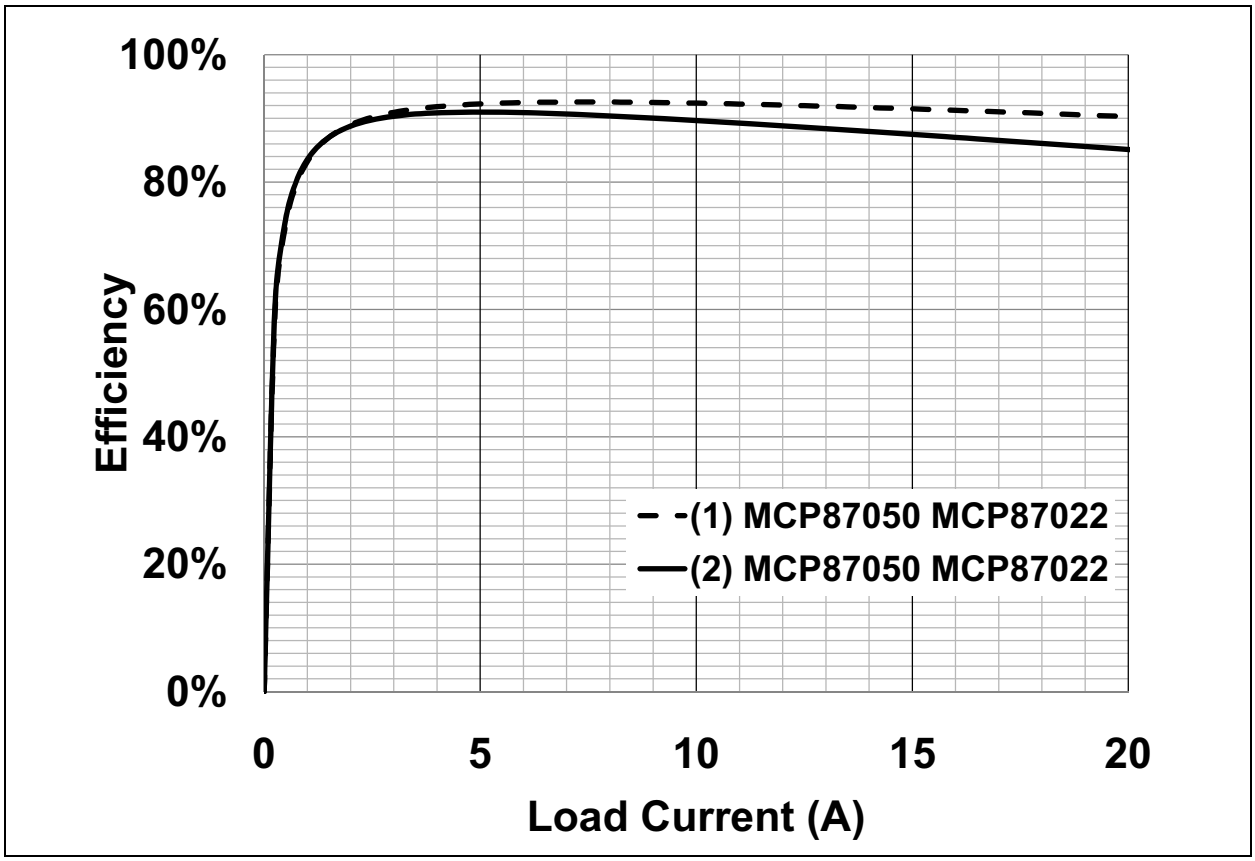

FIGURE B-2: MULTIPLE EFFICIENCY CURVES - EXTRACT FROM GRAPH SHEET.

APPENDIX C: ADDITIONAL EQUATIONS

EQUATION C-1: HIGH-SIDE MOSFET RMS CURRENT

$$I_{DS(RMS)} = \sqrt{\frac{1}{3} \times DC \times \left[\left(I_{OUT} + \frac{I_{RIP}}{2}\right)^2 + \left(I_{OUT} - \frac{I_{RIP}}{2}\right) \times \left(I_{OUT} + \frac{I_{RIP}}{2}\right) + \left(I_{OUT} - \frac{I_{RIP}}{2}\right)^2\right]}$$

Where:

DC = Duty Cycle

I_{OUT} = Output Current

I_{RIP} = Ripple Current

EQUATION C-2: LOW-SIDE MOSFET RMS CURRENT

$$I_{DS(RMS)} = \sqrt{\frac{1}{3} \times (1 - DC) \times \left[\left(I_{OUT} + \frac{I_{RIP}}{2}\right)^2 + \left(I_{OUT} - \frac{I_{RIP}}{2}\right) \times \left(I_{OUT} + \frac{I_{RIP}}{2}\right) + \left(I_{OUT} - \frac{I_{RIP}}{2}\right)^2\right]}$$

EQUATION C-3: RIPPLE CURRENT

$$I_{RIP} = \frac{(V_{IN} - V_{OUT}) \times DC}{L \times F_{SW}}$$

Where:

L = Inductance

Note the following details of the code protection feature on Microchip devices:

- Microchip products meet the specification contained in their particular Microchip Data Sheet.
- Microchip believes that its family of products is one of the most secure families of its kind on the market today, when used in the intended manner and under normal conditions.
- There are dishonest and possibly illegal methods used to breach the code protection feature. All of these methods, to our knowledge, require using the Microchip products in a manner outside the operating specifications contained in Microchip's Data Sheets. Most likely, the person doing so is engaged in theft of intellectual property.
- Microchip is willing to work with the customer who is concerned about the integrity of their code.
- Neither Microchip nor any other semiconductor manufacturer can guarantee the security of their code. Code protection does not mean that we are guaranteeing the product as "unbreakable."

Code protection is constantly evolving. We at Microchip are committed to continuously improving the code protection features of our products. Attempts to break Microchip's code protection feature may be a violation of the Digital Millennium Copyright Act. If such acts allow unauthorized access to your software or other copyrighted work, you may have a right to sue for relief under that Act.

Trademarks

Printed on recycled paper.

ISBN: 978-1-62076-557-5

QUALITY MANAGEMENT SYSTEM
CERTIFIED BY DNV
ISO/TS 16949

Microchip received ISO/TS-16949:2009 certification for its worldwide headquarters, design and wafer fabrication facilities in Chandler and Tempe, Arizona; Gresham, Oregon and design centers in California and India. The Company's quality system processes and procedures are for its PIC® MCUs and dsPIC® DSCs, KEELOQ® code hopping devices, Serial EEPROMs, microperipherals, nonvolatile memory and analog products. In addition, Microchip's quality system for the design and manufacture of development systems is ISO 9001:2000 certified.

Worldwide Sales and Service

AMERICAS

Corporate Office
2355 West Chandler Blvd.
Chandler, AZ 85224-6199
Tel: 480-792-7200
Fax: 480-792-7277
Technical Support:
http://www.microchip.com/support
Web Address:
www.microchip.com

Atlanta
Duluth, GA
Tel: 678-957-9614
Fax: 678-957-1455

Boston
Westborough, MA
Tel: 774-760-0087
Fax: 774-760-0088

Chicago
Itasca, IL
Tel: 630-285-0071
Fax: 630-285-0075

Cleveland
Independence, OH
Tel: 216-447-0464
Fax: 216-447-0643

Dallas
Addison, TX
Tel: 972-818-7423
Fax: 972-818-2924

Detroit
Farmington Hills, MI
Tel: 248-538-2250
Fax: 248-538-2260

Indianapolis
Noblesville, IN
Tel: 317-773-8323
Fax: 317-773-5453

Los Angeles
Mission Viejo, CA
Tel: 949-462-9523
Fax: 949-462-9608

Santa Clara
Santa Clara, CA
Tel: 408-961-6444
Fax: 408-961-6445

Toronto
Mississauga, Ontario, Canada
Tel: 905-673-0699
Fax: 905-673-6509

ASIA/PACIFIC

Asia Pacific Office
Suites 3707-14, 37th Floor
Tower 6, The Gateway
Harbour City, Kowloon
Hong Kong
Tel: 852-2401-1200
Fax: 852-2401-3431

Australia - Sydney
Tel: 61-2-9868-6733
Fax: 61-2-9868-6755

China - Beijing
Tel: 86-10-8569-7000
Fax: 86-10-8528-2104

China - Chengdu
Tel: 86-28-8665-5511
Fax: 86-28-8665-7889

China - Chongqing
Tel: 86-23-8980-9588
Fax: 86-23-8980-9500

China - Hangzhou
Tel: 86-571-2819-3187
Fax: 86-571-2819-3189

China - Hong Kong SAR
Tel: 852-2401-1200
Fax: 852-2401-3431

China - Nanjing
Tel: 86-25-8473-2460
Fax: 86-25-8473-2470

China - Qingdao
Tel: 86-532-8502-7355
Fax: 86-532-8502-7205

China - Shanghai
Tel: 86-21-5407-5533
Fax: 86-21-5407-5066

China - Shenyang
Tel: 86-24-2334-2829
Fax: 86-24-2334-2393

China - Shenzhen
Tel: 86-755-8203-2660
Fax: 86-755-8203-1760

China - Wuhan
Tel: 86-27-5980-5300
Fax: 86-27-5980-5118

China - Xian
Tel: 86-29-8833-7252
Fax: 86-29-8833-7256

China - Xiamen
Tel: 86-592-2388138
Fax: 86-592-2388130

China - Zhuhai
Tel: 86-756-3210040
Fax: 86-756-3210049

ASIA/PACIFIC

India - Bangalore
Tel: 91-80-3090-4444
Fax: 91-80-3090-4123

India - New Delhi
Tel: 91-11-4160-8631
Fax: 91-11-4160-8632

India - Pune
Tel: 91-20-2566-1512
Fax: 91-20-2566-1513

Japan - Osaka
Tel: 81-66-152-7160
Fax: 81-66-152-9310

Japan - Yokohama
Tel: 81-45-471- 6166
Fax: 81-45-471-6122

Korea - Daegu
Tel: 82-53-744-4301
Fax: 82-53-744-4302

Korea - Seoul
Tel: 82-2-554-7200
Fax: 82-2-558-5932 or
82-2-558-5934

Malaysia - Kuala Lumpur
Tel: 60-3-6201-9857
Fax: 60-3-6201-9859

Malaysia - Penang
Tel: 60-4-227-8870
Fax: 60-4-227-4068

Philippines - Manila
Tel: 63-2-634-9065
Fax: 63-2-634-9069

Singapore
Tel: 65-6334-8870
Fax: 65-6334-8850

Taiwan - Hsin Chu
Tel: 886-3-5778-366
Fax: 886-3-5770-955

Taiwan - Kaohsiung
Tel: 886-7-213-7828
Fax: 886-7-330-9305

Taiwan - Taipei
Tel: 886-2-2508-8600
Fax: 886-2-2508-0102

Thailand - Bangkok
Tel: 66-2-694-1351
Fax: 66-2-694-1350

EUROPE

Austria - Wels
Tel: 43-7242-2244-39
Fax: 43-7242-2244-393

Denmark - Copenhagen
Tel: 45-4450-2828
Fax: 45-4485-2829

France - Paris
Tel: 33-1-69-53-63-20
Fax: 33-1-69-30-90-79

Germany - Munich
Tel: 49-89-627-144-0
Fax: 49-89-627-144-44

Italy - Milan
Tel: 39-0331-742611
Fax: 39-0331-466781

Netherlands - Drunen
Tel: 31-416-690399
Fax: 31-416-690340

Spain - Madrid
Tel: 34-91-708-08-90
Fax: 34-91-708-08-91

UK - Wokingham
Tel: 44-118-921-5869
Fax: 44-118-921-5820

10/26/12